Electronic Supplementary Material (ESI) for Journal of Materials Chemistry A.

Supporting Information

Amorphous NiFe(oxy)hydroxide Nanosheets Integrated Partially Exfoliated Graphite Foil for High Efficiency Oxygen Evolution Reaction

Yin-Jian Ye,[a] Ning Zhang[b] and Xiao-Xia Liu*[a]

[a] Department of Chemistry, Northeastern University, Shenyang, 110819, China

[b] Institute of Advance Material Technology, Northeastern University, Shenyang, 110819, China.

*Corresponding author: Xiao-Xia Liu, xxliu@mail.neu.edu.cn

List of supporting tables

Table S1. Comparison of the electrocatalytic performance of the NiFe/EG catalyst present in this work with some representative Ni-Fe bimetallic OER catalysts reported recently.

	Electrolyte	Current density (i) (mA cm^{-2})	η (mv) at correspon-ding i	Tafel slope (mv/dec)	Duration time (h)	Ref.
NiFe/EG	1 M KOH	10 500	214 251	21.2	100 48	This work
	0.1 M KOH	10	248	31.0	—	
NiFe/NF	1 M KOH	100	370	28	10	[31]
	10 M KOH	500	240	—	2	
NiFe/$NiCo_2O_4$/ NF	1 M KOH	50	310	38.8	11	[32]
Ni-Fe-OH@Ni_3S_2/NF	1 M KOH	10 500	165 530	93	 50	[33]
$Ni_{50}Fe_{50}$-DAT/ NF	1 M NaOH	100	300	—	72	[34]
NiFe-C/NF	1 M KOH	60	275	30	100	[35]
NiFe-LDH/MWCNT	1 M KOH	40	240	33.3	24	[38]
NiFe-LDH/$Co_{0.85}Se$/EG	1 M KOH	200	270	57	10	[40]
NiFe-LDH/NF	1 M KOH	10	224	52.8	50	[42]
$Ni_{0.71}Fe_{0.29}(OH)_x$/ graphite	0.1 M KOH	10	296	58	24	[27]
Ni-Fe LDH/3D-ErGO	1 M KOH	10	259	39	2	[51]
porous Ni-Fe	0.1 M KOH	10	328	42	12	[15]
NiFe-LDH/CQD	1 M KOH	10	235	30	0.83	[17]
NiFe-LDH/CNT	1 M KOH	10	~250	31	0.28	[18]
$Ni_{2/3}Fe_{1/3}$-LDH/ rGO	1 M KOH	10	210	40	10	[19]
NiFe-LDH/GO	1 M KOH	10	210	39	1.3	[20]
NiFe-LDH/ N-Graphene	0.1 M KOH	10	337	45	3	[21]

Table S2. Comparison of the electrocatalytic performance of the NiFe/EG catalyst reported in this work with comercial noble metal based OER catalysts reported recently.

Sample	Electrolyte	Current density (i) (mA cm^{-2})	η (mv) at correspon-ding *i*	Tafel slope (mv/dec)	Ref.
Ir/C on GCE[1]	0.1 M KOH	10	410	54	[21]
Ir/C on Ni foam	1 M KOH	10	490	145	[42]
IrO_2 on GCE[1]	1 M KOH	10	370	64	[12]
IrO_2 on RDE[2]	1 M KOH	10	470	61	[51]
IrO_2 on RDE[2]	1 M KOH	10	360	42.8	[38]
IrO_2 on Ni foam	1 M KOH	10	290	78.5	[9]
IrO_2 on Ni foam	1 M KOH	355	570	-----	[33]
RuO_2 on graphite	0.1 M KOH	10	350	61	[27]
RuO_2 on graphite	0.1 M KOH	10	497	86	[28]
RuO_2 on GCE[1]	1 M KOH	10	320	54.4	This work
NiFe/EG	1 M KOH	10	214	21.2	This work
	0.1 M KOH	10	248	31.0	

[1]GCE (Glassy Carbon Electrode)
[2]RDE (Ring Disk Electrode)

Table S3. Ni:Fe atomic ratios

sample	Ni:Fe precursor ratio in electrolyte	Ni:Fe ratio in NiFe/EG-1.2V electrode
NiFe8:1/EG-1.2V	8:1	89.7:10.3
NiFe4:1/EG-1.2V	4:1	83.3:16.7
NiFe2:1/EG-1.2V	2:1	75.4:24.6
NiFe1:1/EG-1.2V	1:1	44.3:55.7

List of supporting figures

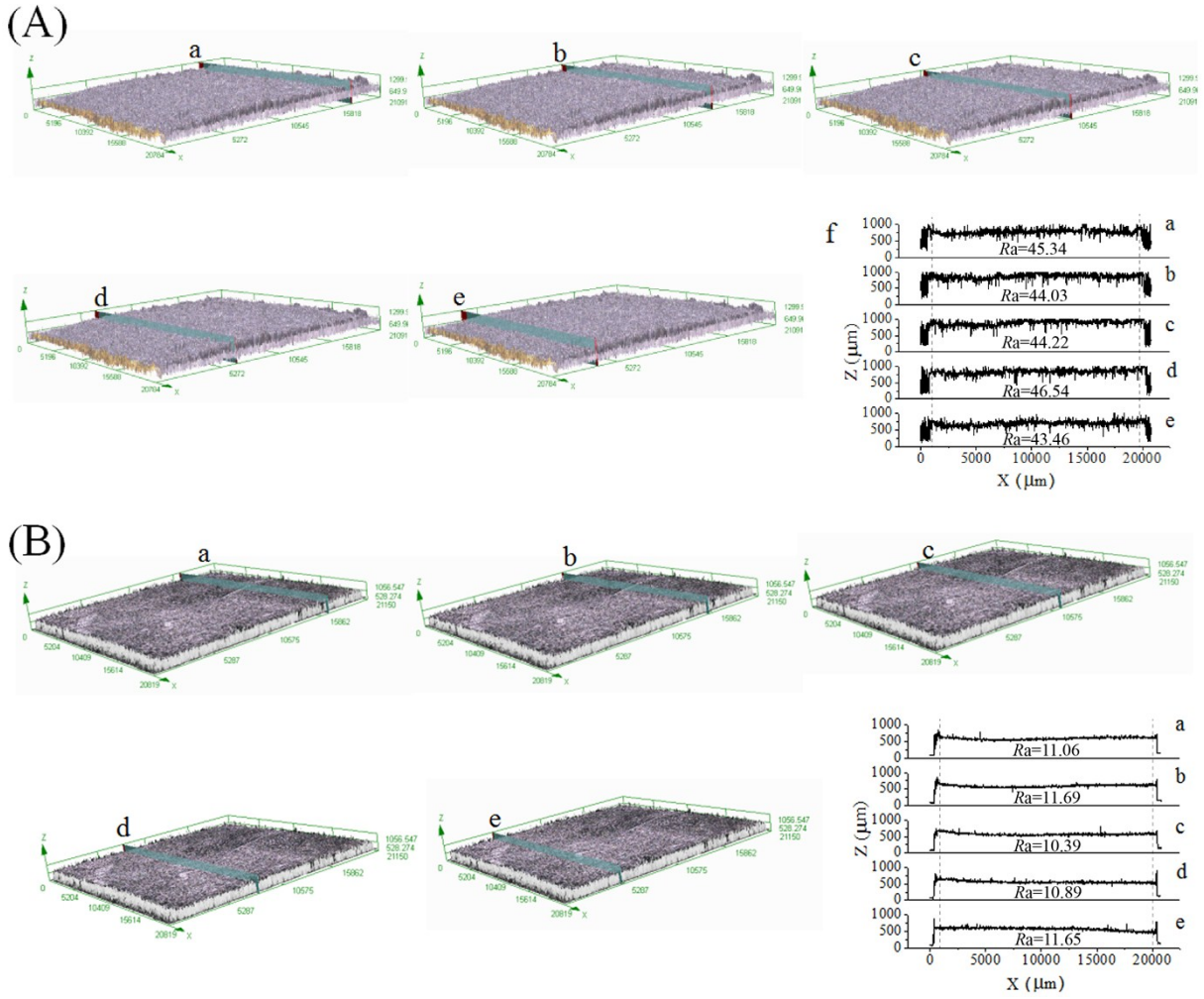

Figure S1. Confocal laser scanning microscope images of EG (A: a-e) and G (B: a-e) together with the heights along the y direction in different positions as labelled in a-e (f).

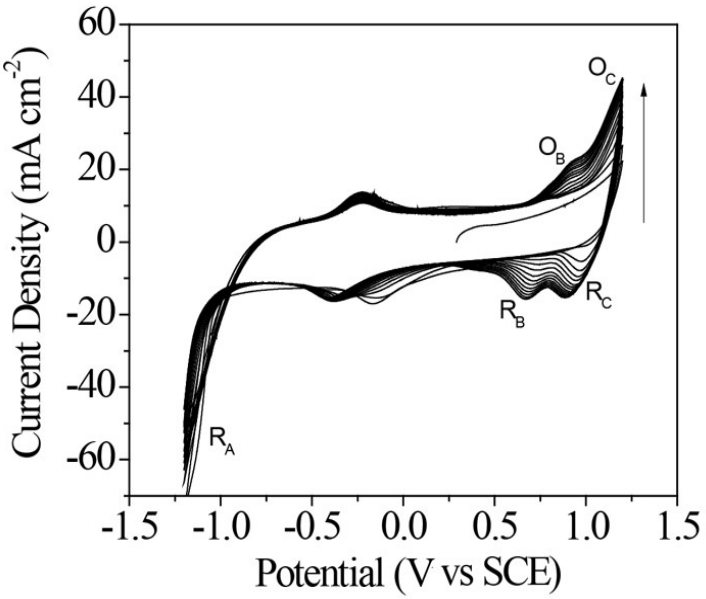

Figure S2. Cyclic voltammograms (CV) during the electrodeposition of NiFe(oxy)hydroxide species on EG substrate.

Reactions involved:

$$R_A: \quad NO_3^- + 7H_2O + 8e^- \rightarrow NH_4^+ + 10OH^- \tag{1}$$

$$xNi^{2+} + yFe^{3+} + (2x+y)OH^- \rightarrow Ni_xFe_yOH_{(2x+3y)} \tag{2}$$

$$O_B/R_B: \quad Ni(OH)_2(s) \leftrightarrow NiOOH(s) + H^+ + e^- \tag{3}$$

$$O_C/R_C: \quad Ni^{2+}(aq) + 2H_2O \leftrightarrow NiOOH(s) + 3H^+ + e^- \tag{4}$$

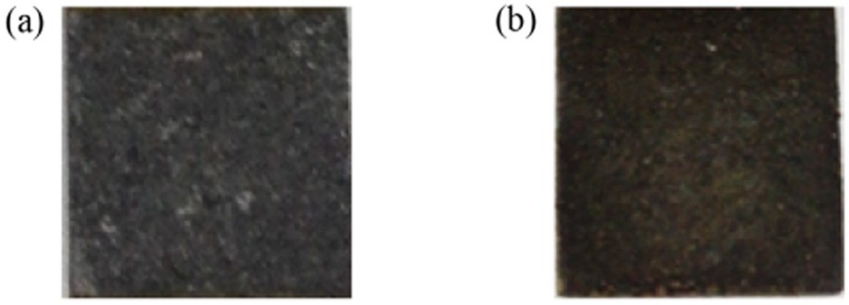

Figure S3. Photographs of the as-prepared (a) EG and (b) NiFe2:1/EG-1.2V electrodes.

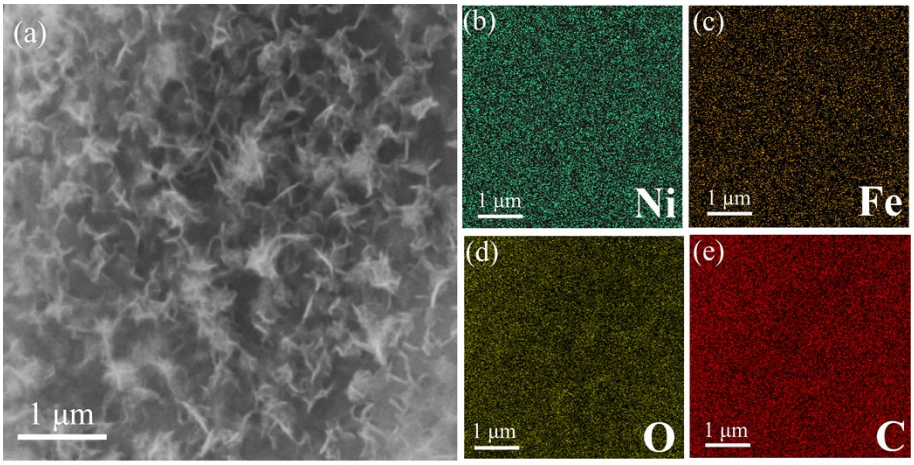

Figure S4. SEM image (a) of NiFe2:1/EG-1.2V and corresponding EDS mapping images for Ni (b), Fe (c), O (d) and C (e).

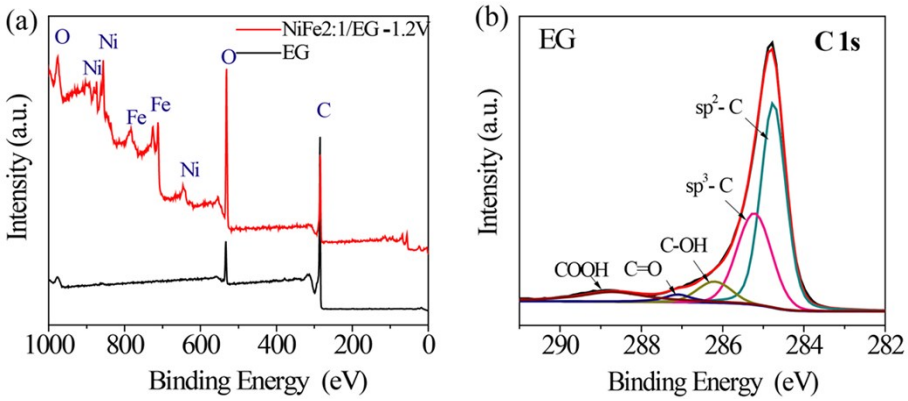

Figure S5. (a) XPS survey spectra of EG (black) and NiFe2:1/EG-1.2V electrode (red). (b) Detailed fits of the C 1s of EG.

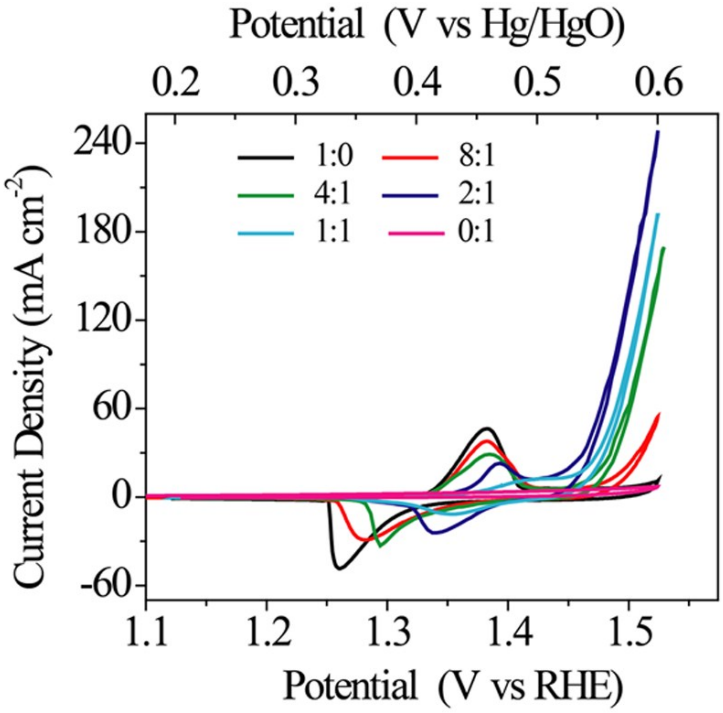

Figure S6. CV curves of the NiFe/EG-1.2V electrodes prepared from the mixed nitrate precursors with different Ni/Fe ratios (1:0, 8:1, 4:1, 2:1, 1:1, 0:1)

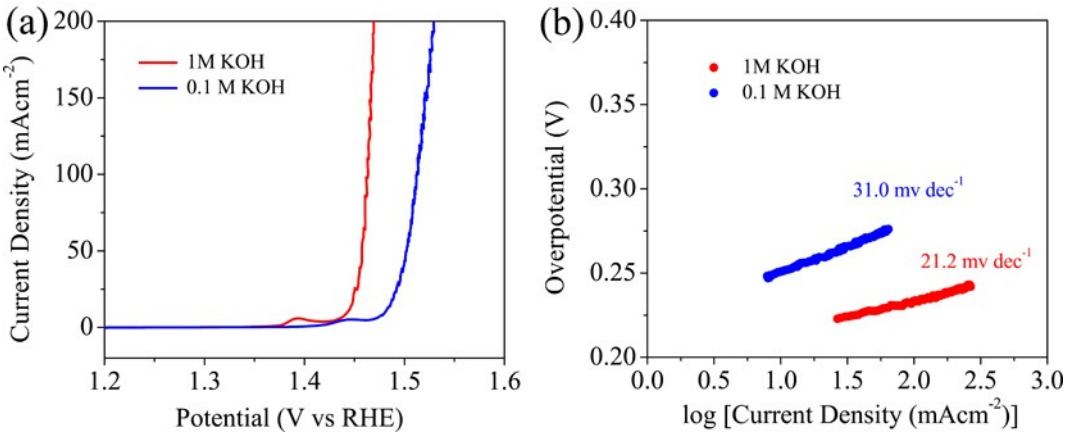

Figure S7. (a) *iR*-corrected LSV curves of NiFe/EG-1.2V electrode in KOH solutions with different concentrations and (b) the corresponding Tafel plots of overpotential versus log (*i*) derived from (a)

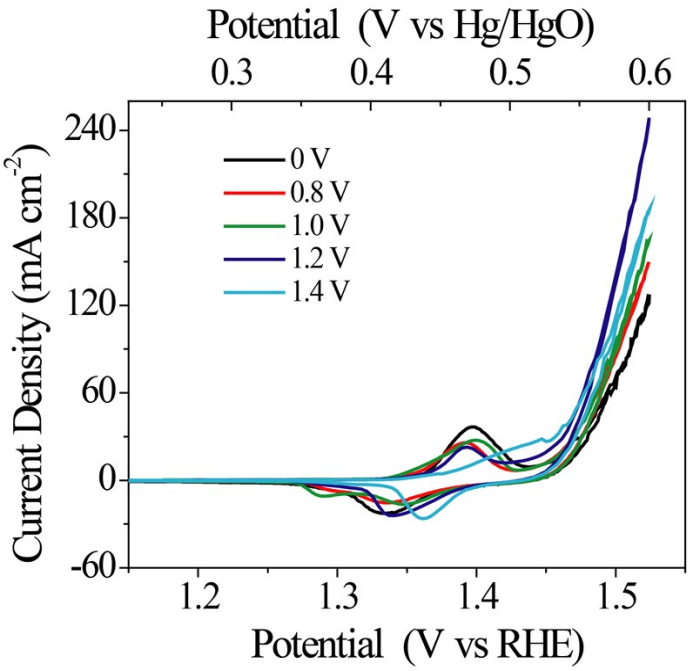

Figure S8. CV curves of the NiFe2:1/EG electrodes prepared from potential dynamic scans between -1.2 V vs. SCE and different upper potential cutoffs (0 V, 0.8 V, 1.0 V, 1.2 V, 1.4 V).

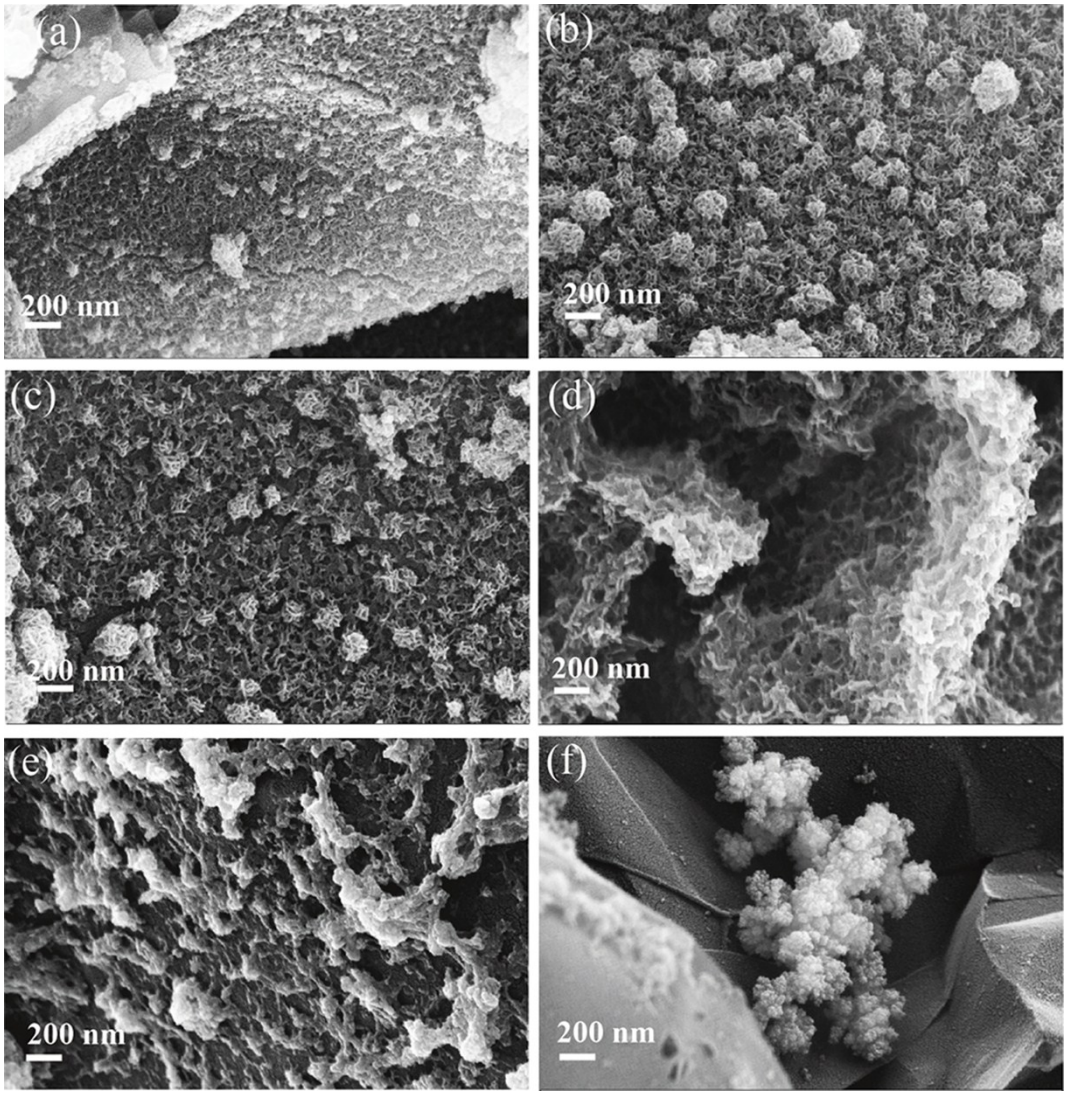

Figure S9. SEM images of (a) Ni/EG-1.2V, (b) NiFe8:1/EG-1.2V, (c) NiFe4:1/EG-1.2V, (d) NiFe2:1/EG-1.2V, (e) NiFe1:1/EG-1.2V and (f) Fe/EG-1.2V electrodes.

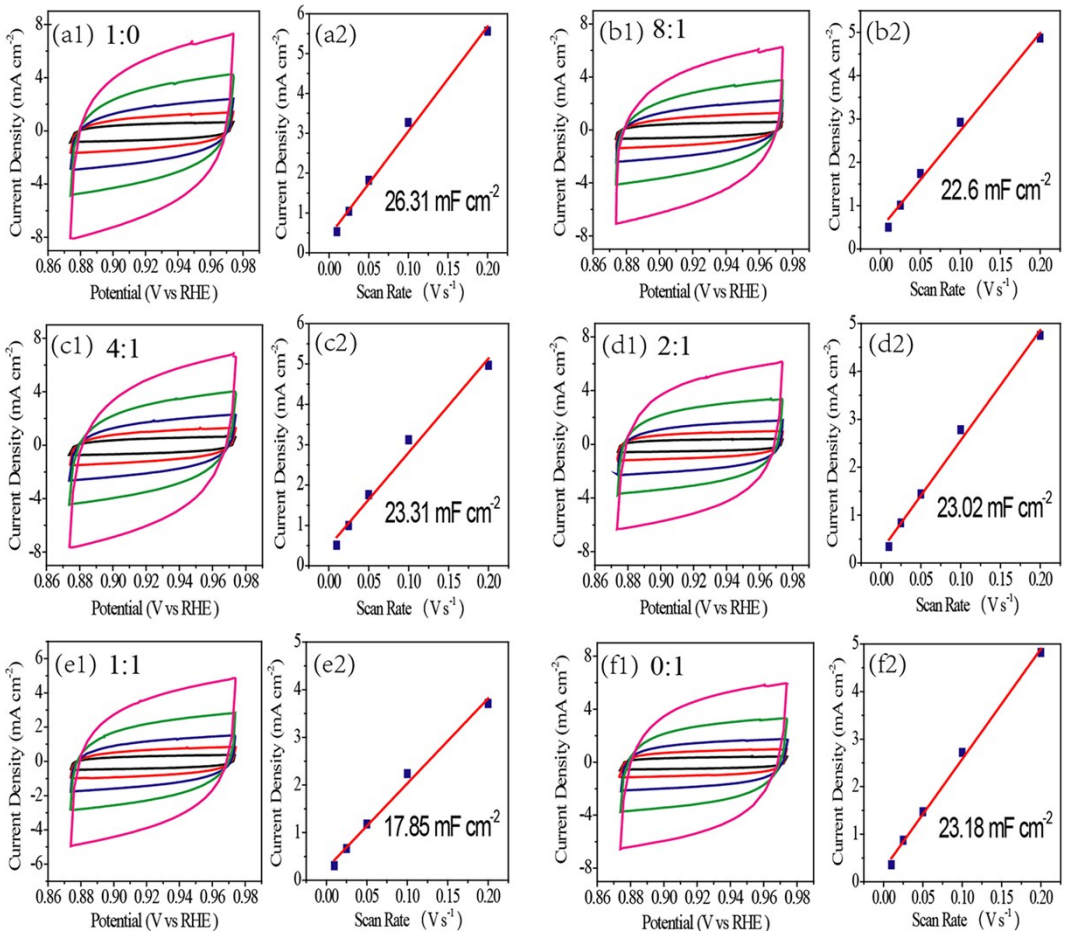

Figure S10. CV curves of (a1) Ni/EG-1.2V, (b1) NiFe8:1/EG-1.2V, (c1) NiFe4:1/EG-1.2V, (d1) NiFe2:1/EG-1.2V, (e1) NiFe1:1/EG-1.2V and (f1) Fe/EG-1.2V electrodes measured in the non-Faradaic region at the following scan rates: 10 mV s^{-1} (black line), 25 mV s^{-1} (red line), 50 mV s^{-1} (blue line), 100 mV s^{-1} (green line), 200 mV s^{-1} (pink line); (a2)-(f2) The linear relationship of current densities at 0.924 V vs. RHE with scan rates allows to estimate the double layer capacitance (C_{dl}), which directly related to EASA, from the slope.

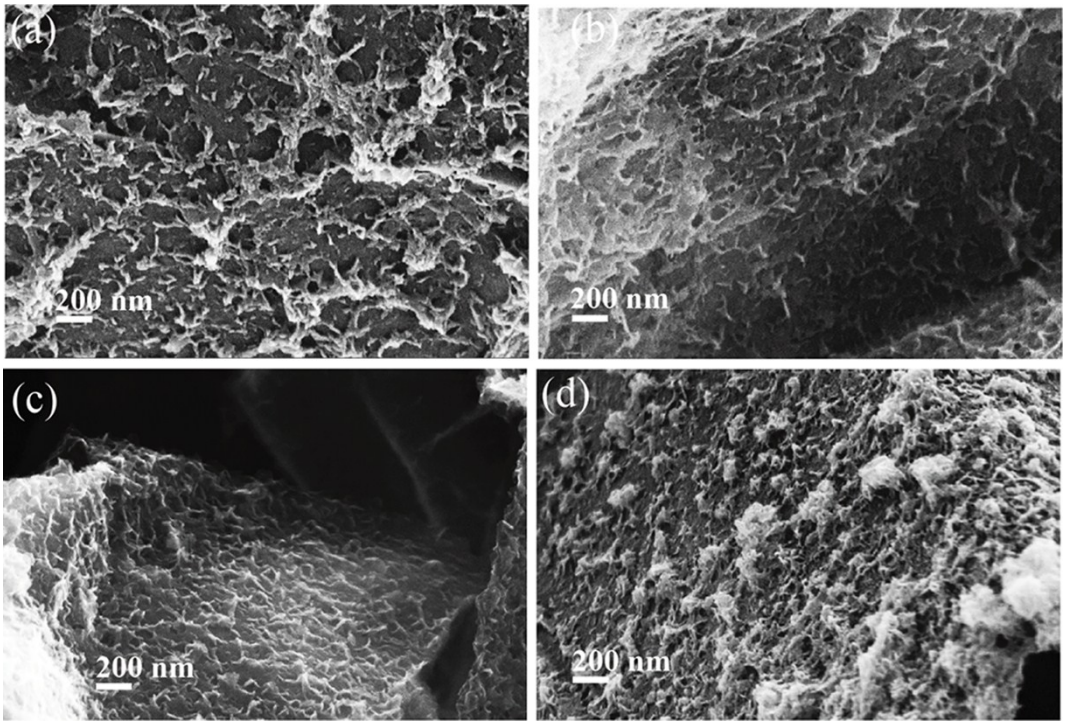

Figure S11. SEM images of (a) NiFe2:1/EG-0V, (b) NiFe2:1/EG-0.8V, (c) NiFe2:1/EG-1.0V and (d) NiFe2:1/EG-1.4V electrodes.

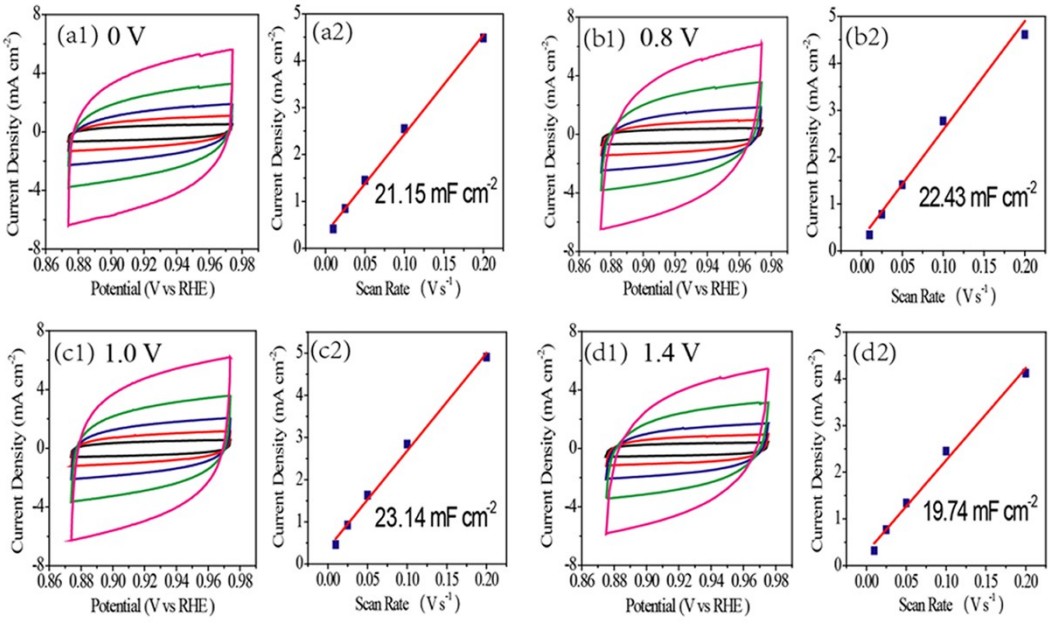

Figure S12. CV curves of (a1) NiFe2:1/EG-0V, (b1) NiFe2:1/EG-0.8V, (c1) NiFe2:1/EG-1.0V and (d1) NiFe2:1/EG-1.4V electrodes measured in the non-Faradaic region at the following scan rates: 10 mV s^{-1} (black line), 25 mV s^{-1} (red line), 50 mV s^{-1} (blue line), 100 mV s^{-1} (green line), 200 mV s^{-1} (pink line); (a2)-(d2) The linear relationship of current densities at 0.924 V vs. RHE with scan rates allows to estimate the double layer capacitance (C_{dl}), which directly relates to EASA, from the slope.

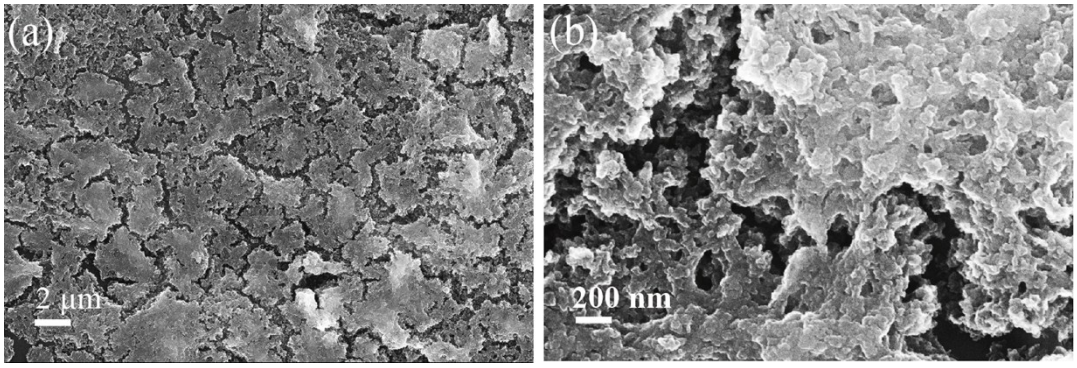

Figure S13. SEM images of the NiFe2:1/G-1.2V electrode.

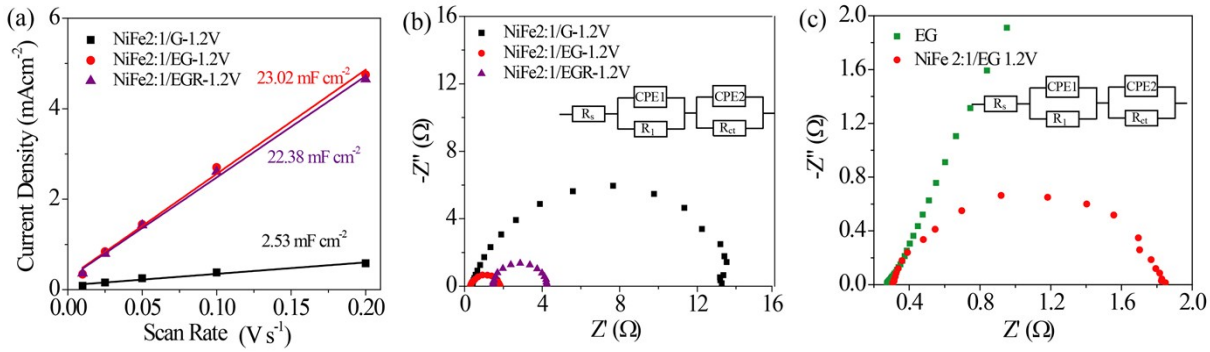

Figure S14. (a) Plots of current densities at 0.924 V vs. RHE with various scan rates in CV curves in the non-Faradaic region of NiFe2:1/G-1.2V, NiFe2:1/EG-1.2V and NiFe2:1/EGR-1.2V electrodes for the estimation of double layer capacitance (C_{dl}). (b) Nyquist plots of the NiFe2:1/G-1.2V, NiFe2:1/EG-1.2V and NiFe2:1/EGR-1.2V electrodes conducted in a frequency range of 10 mHz to 20 kHz at potential of 1.504 V vs. RHE. (c) Nyquist plots of EG and the NiFe2:1/EG-1.2V electrode conducted in a frequency range of 10 mHz to 20 kHz at potential of 1.504 V vs. RHE.

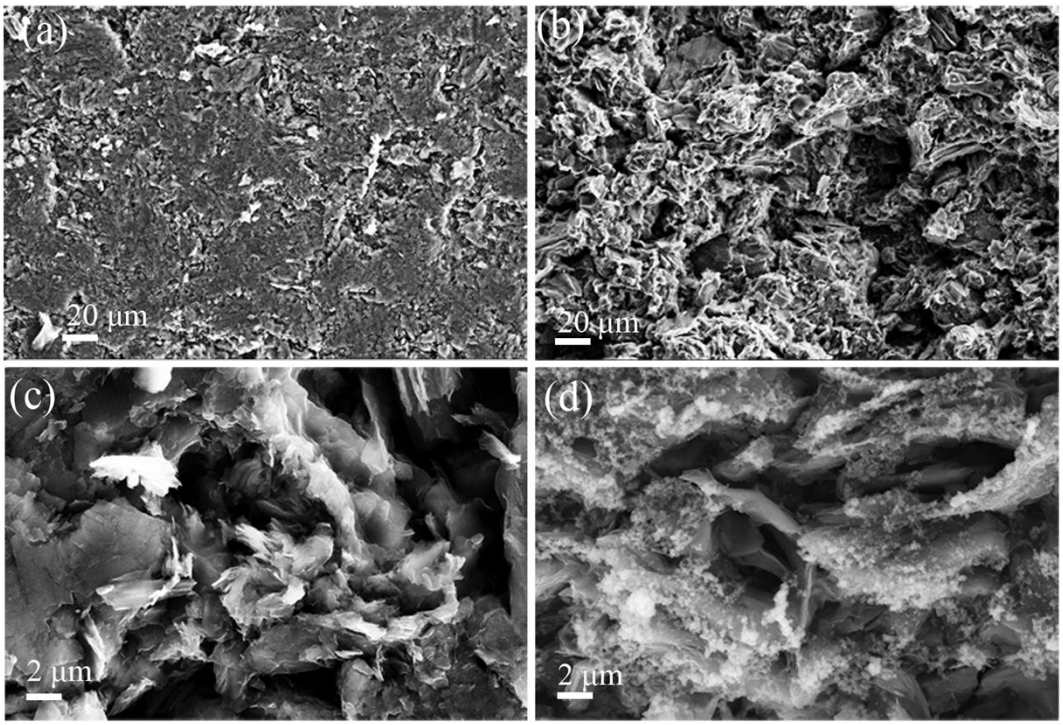

Figure S15. SEM images of GR (a), EGR (b and c) and NiFe2:1/EGR-1.2V (d).

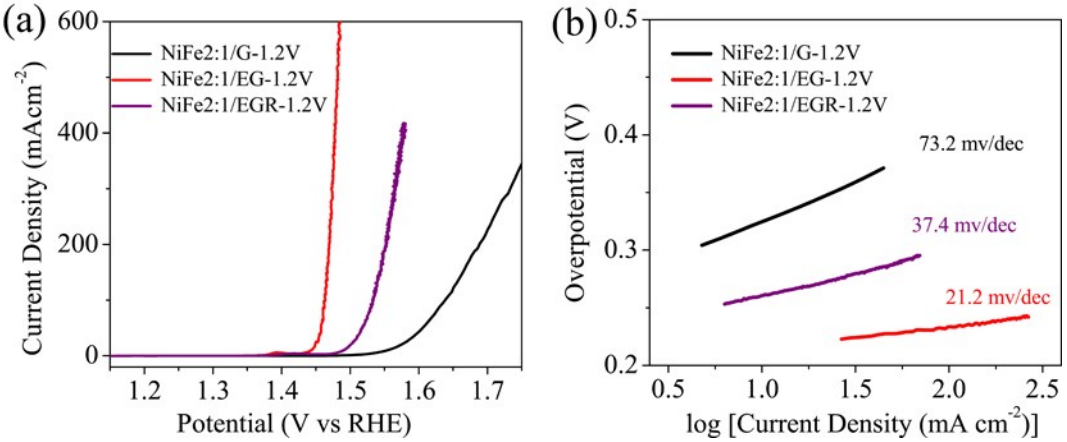

Figure S16. (a) The *iR*-corrected LSV curves of NiFe2:1/EG-1.2V, NiFe2:1/EGR-1.2V and NiFe2:1/G-1.2V electrodes. (b) Tafel plots of overpotential versus log (*i*) derived from (a).